Role of stable eigenmodes in saturated local plasma turbulence

P. W. Terry, D. A. Baver, and Sangeeta Gupta
University of Wisconsin—Madison, Madison, Wisconsin 53706

(Received 31 March 2005; accepted 5 January 2006; published online 10 February 2006)

The excitation of stable eigenmodes in unstable plasma turbulence, previously documented in collisionless trapped electron mode turbulence, is shown to be a generic behavior of local (quasihomogeneous) systems. A condition is derived to indicate when such excited eigenmodes achieve a sufficient level in saturation to affect the turbulence, and produce changes in saturation levels, instability drive, and transport. The condition is shown to be consistent with the results of collisionless and dissipative trapped electron turbulence, and is further illustrated by an entirely different model describing simple ion turbulence driven by the ion temperature gradient. The condition suggests that all eigenmodes of the ion model affect saturation, but none dominates. This is consistent with the results of simulations, which show nonlinear modifications to eigenmode structure, growth rate, and transport that occur intermittently in time, despite fixed driving gradients. © *2006 American Institute of Physics*. [DOI: 10.1063/1.2168453]

I. INTRODUCTION

Turbulence in confined plasmas is driven by instabilities. At finite amplitude, the drive need not be given by the linear growth rate. However, this is often assumed, and the notion is pervasive in the conceptualization of instability-driven plasma turbulence. It is recognized, of course, that instability is not necessarily linear. Nonlinear instability is a familiar concept in dynamical systems,[1] and has been explored in a number of plasma models.[2–7] These studies have generally focused on subcritical instability, i.e., instability when the system is below the linear threshold, but finite amplitude allows free energy to be released. Above the linear threshold (supercritical instability), the growth rate can also be modified by finite amplitude. While methods have been developed to treat this situation, these methods have difficulties that have generally gone unrecognized.

Attempts to deal with the supercritical situation largely fall into two categories. One is the concept of secondary instability, where the linear instability creates a finite-amplitude structure that is itself subject to further instability.[8–11] Once a structure is postulated, secondary instability can be treated with linearized perturbations about the primary structure. Most descriptions of zonal flow excitation effectively fall into this category. A second approach involves an ad hoc "nonlinear" eigenmode calculation, in which an eigenmode is calculated in the presence of nonlinear effects that are represented by linear surrogates.[12,13] Anomalous viscosities fall into this category if the anomalous coefficient is prescribed and not subject to active dynamical interaction with the turbulence. While the eigenmodes so calculated differ from the linear eigenmode, they remain essentially linear, modified by dissipation that is anomalously large relative to collisional values.

The problem with the above procedures is that, in any complete basis spanning the space of allowed collective motions of the system, they correspond to a partial sampling, and one whose projection on the complete basis is undetermined. At issue are eigenmode branches that are linearly damped for all wave numbers, and therefore usually ignored, but susceptible to nonlinear excitation. The ad hoc nature of the above procedures makes it unclear as to whether the fluctuation structures they select or impose are consistent with fluctuations excited by the nonlinearity from a complete basis set. Even though these structures modify the linearly unstable eigenmode, they cannot represent a complete response, if, as in the case of zonal flows, they are a lower dimensional manifold of the complete space. Moreover, they remain essentially linear, or can be formulated in a straightforward fashion from Fourier modes on the unstable eigenmode branch, albeit over an extended range.

The participation of stable eigenmode branches in turbulent dynamics is not academic. Multiple stable eigenmode branches are excited and interact in three-dimensional (3D) rotating,[14] rotating stratified,[15] and magnetohydrodynamic (MHD) turbulence.[16] In plasma microturbulence, this possibility was suggested[17] but not explored until recently when it was shown that a damped eigenmode is excited in collisionless trapped electron mode (CTEM) turbulence, and plays a major role in the dynamics.[18,19] A stable eigenmode has also been invoked to explain the observed isotope scaling of transport in the Columbia Linear Machine.[20] The CTEM problem shows that excitation of a damped eigenmode can make radical changes to the turbulence. These include the creation of an unconventional inverse cascade,[21] a nonlinear particle pinch,[22] and the introduction of a new saturation channel to zonal modes on the stable eigenmode branch.[23,24] The zonal modes that saturate the instability are robustly damped by collisional detrapping of trapped electrons, and are distinct (linearly independent) from the familiar zonal flow structures associated with the potential and a vanishing adiabatic density.[25] The familiar zonal flows constitute the zonal component of the unstable eigenmode branch, and do not saturate the turbulence in the CTEM model because the zonal wave number $k_y=0$ is marginally stable. Any treatment that singles out and restricts itself to these zonal flows misses

zonal modes on the second eigenmode branch and their potent effect on saturation.

Given the significance of these effects, it is important to determine whether they are unique to the CTEM model or occur more generally. It is also important to understand the physics by which stable eigenmodes affect saturation and transport, and what conditions are required. This paper derives general conditions applicable to any local fluid model above the linear instability threshold, such that the saturated state and instability drive are significantly modified by stable eigenmodes. To test the validity and usefulness of these conditions, we will apply them to the CTEM model, where a reasonably complete picture of the physics of a stable eigenmode already exists. However, it is also important to assess the value of these conditions under more general circumstances, for example situations with multiple stable eigenmode branches, including marginally stable eigenmodes. Moreover, it is important to sample models that are different from CTEM to begin assessing the generality of stable eigenmode excitation in unstable plasmas.

To this end, we introduce a simple ion drift wave model that is nonetheless more complex than the CTEM model. In addition to unstable and robustly damped eigenmodes, it has a marginally stable eigenmode. This allows us to study whether weakly damped or marginally stable eigenmodes have an advantage over robustly damped eigenmodes, a question of relevance to zonal flows, which are usually considered to be weakly damped. The physics of the couplings in the ion model are completely different from those of CTEM. Therefore, the discovery in this model of damped eigenmode effects is an important and nontrivial (but not final) step toward determining if such effects are present in plasma turbulence generally. Finally, the model retains sufficient simplicity to guarantee the transparency needed for initial studies of nonlinear effects that have otherwise gone undetected. Although the model relates primitively to ion temperature gradient (ITG) turbulence, the relationship is incidental. Modeling ITG turbulence requires additional effects, and is not the point of this paper.

We show that the nonlinear excitation of stable eigenmodes is universal, and drives exponential growth, provided initial levels are infinitesimal. A heuristic analysis yields a simple condition such that a stable eigenmode affects saturation under generic mode coupling. The condition is consistent with behavior in both the CTEM and ion models. For $E\times B$ advection the condition is tied to correlations that govern the growth rate, ensuring that growth rates are modified in saturation. We also observe novel effects in the ion model. The most striking is the appearance of intrinsic temporal variability of growth rates and transport fluxes in fixed-gradient turbulence. The paper is organized as follows: In Sec. II we present and discuss the basic model. In Sec. III we examine damped and marginally stable eigenmode excitation and derive the condition that indicates when these eigenmodes affect saturation. In Sec. IV we show how the condition relates to the instability drive. Section V gives conclusions and implications.

II. THE ION MODEL

The simple fluid model for turbulence driven by ion temperature gradient employed in this paper is based on the following equations:

$$(1+k^2)\frac{\partial\phi}{\partial t} - ik_y v_D\phi(\hat{\eta}k^2-1) + ik_z u_\parallel = -\sum_{k'}(k'\times\hat{z}\cdot k)\phi_{k'}\phi_{k-k'}k'^2 \equiv (1+k^2)N_\phi, \tag{1}$$

$$\frac{\partial u_\parallel}{\partial t} + ik_z\phi + ik_z p = -\sum_{k'}(k'\times\hat{z}\cdot k)\phi_{k'}u_{\parallel k-k'} \equiv N_{u_\parallel}, \tag{2}$$

$$\frac{\partial p}{\partial t} + ik_y v_D\hat{\eta}\phi = -\sum_{k'}(k'\times\hat{z}\cdot k)\phi_{k'}p_{k-k'} \equiv N_p, \tag{3}$$

where $v_D\equiv(cT_e/eB)d(\ln n_0)/dx$ is the drift velocity, $\hat{\eta}=(1+\eta_i)/\tau$, $\eta_i=d(\ln T_i)/d(\ln n_0)$ is the ratio of temperature to density gradient scale lengths, $\tau\equiv T_e/T_i$ is the ratio of electron to ion temperature, and ϕ, $u_\parallel$, and p are the Fourier amplitudes of potential, parallel ion flow, and ion pressure. These are normalized according to $\phi\equiv e\Phi/T_e$, $u_\parallel\equiv\tilde{v}_{\parallel i}/c_s$, and $p\equiv[\tilde{p}_i/\langle P_{i0}\rangle](T_i/T_e)$, where $P_i=\langle P_{i0}\rangle+\tilde{p}_i$. Length scales are normalized to $\rho_s=(cT_e/eB)(m_i/T_e)^{1/2}$. In solving Eqs. (1)–(3), k_z is chosen to be a constant. The reality condition that leads to the parity constraint $\psi(-k)=\psi^*(k)$ dictates that this constant change sign when k maps to negative values.

The linear dispersion relation for normal modes is

$$\omega^3(1+k^2)+\omega^2\omega_*(\hat{\eta}k^2-1)-\omega k_z^2-\omega_* k_z^2\hat{\eta}=0, \tag{4}$$

where $\omega_*=k_y v_D$. This polynomial can be solved for the eigenfrequencies using the exact formula for cubic polynomials. Instability occurs for low k_y, where there is a marginally stable propagating mode and a conjugate pair of lower frequency modes, one of which is growing and one of which is damped. To get a sense of the branch structure, this part of the dispersion can be approximated by the balance of the cubic and constant terms in Eq. (4), yielding roots given by

$$\omega_j \approx s_j\left[\frac{\omega_* k_z^2\hat{\eta}}{1+k^2}\right]^{1/3}, \tag{5}$$

where

$$s_2=1, \tag{6}$$

$$s_{1,3}=\left(-\frac{1}{2}\pm i\frac{\sqrt{3}}{2}\right). \tag{7}$$

For higher values of k_y, corresponding to $\omega^2(\hat{\eta}k^2-1)>k_z^2\hat{\eta}$, all three roots are stable, and split between a high-frequency root with $\omega_1\approx-\omega_*(\hat{\eta}k^2-1)/(1+k^2)$ and two roots with frequencies near zero. The spectrum of growth rates is shown in Fig. 1.

There is some arbitrariness in the labeling of the roots across the boundary dividing regions of complex and wholly real solutions because two of the modes are degenerate at

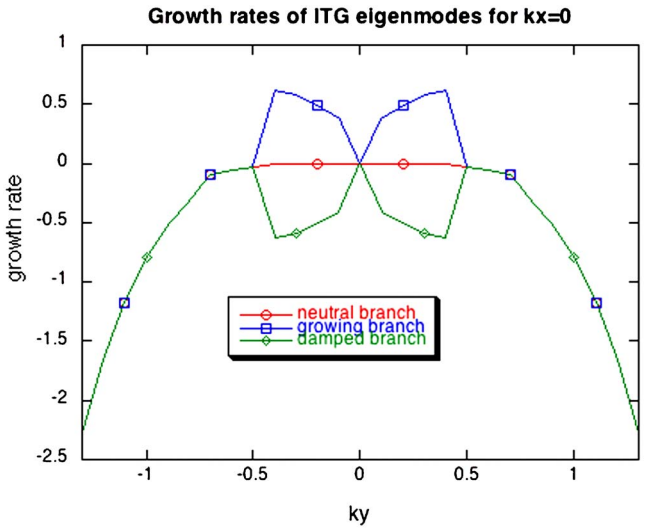

FIG. 1. Imaginary part (growth rates) of three eigenfrequencies of the linear dispersion relation [Eq. (4)] as a function of k_y for $k_x=0$. Growing modes are confined to one branch for $k_y<0.5$. All branches are subjected to hyperviscous-type damping at high k.

this boundary. We adopt the convention of using the same label for the growing branch in the complex-root region as for the high-frequency branch in the real-root region. A convention must be adopted so that consistency is maintained when dynamical solutions for ϕ, $u_\parallel$, and p are projected onto the eigenmodes of the three roots. This procedure is introduced in the next section to enable treatment of the finite-amplitude effects on stability and saturation.

III. EIGENMODE EXCITATION AND HEGEMONY

For systems in which multiple eigenmodes are excited, each excited eigenmode must be tracked. This is accomplished by recasting the basic equations so they describe the nonlinear evolution of each eigenmode amplitude. The expansion of the fields ϕ, $u_\parallel$, and p in the basis set of the linear eigenmodes, which we generally refer to as the eigenmode decomposition, can be written

$$\begin{pmatrix} p \\ u_\parallel \\ \phi \end{pmatrix} = \beta_1 \begin{pmatrix} b_1 \\ a_1 \\ 1 \end{pmatrix} + \beta_2 \begin{pmatrix} b_2 \\ a_2 \\ 1 \end{pmatrix} + \beta_3 \begin{pmatrix} b_3 \\ a_3 \\ 1 \end{pmatrix} = \begin{pmatrix} b_1 & b_2 & b_3 \\ a_1 & a_2 & a_3 \\ 1 & 1 & 1 \end{pmatrix} \begin{pmatrix} \beta_1 \\ \beta_2 \\ \beta_3 \end{pmatrix} \equiv \mathbf{M} \begin{pmatrix} \beta_1 \\ \beta_2 \\ \beta_3 \end{pmatrix}. \tag{8}$$

The original fields ϕ, $u_\parallel$, and p are functions of wave number k and time, hence so are the eigenmode amplitudes β_1, β_2, and β_3. The columns of the matrix $\mathbf{M}$ are the three eigenvectors, normalized so that each eigenvector has a ϕ component of unity. The eigenvector components a_j and b_j are functions of k. They are found in the usual way, replacing $\partial/\partial t$ with $-i\omega_j$ in the linearized form of Eqs. (1)–(3) and solving any two of the three equations for $u_\parallel$ and p in terms of ϕ. We do not write out expressions for $a_j(k)$ and $b_j(k)$ because the exact forms, which we use in numerical solutions, are so algebraically complicated that they offer little insight. Consistent with the labeling introduced in the previous section, β_1, β_2, and β_3 are the amplitudes of the growing, marginal, and damped eigenmodes.

If Eqs. (1)–(3) are written vectorally as $[\dot{p},\dot{u}_\parallel,\dot{\phi}] = \mathbf{D}[p,u_\parallel,\phi]+[N_p,N_{u_\parallel},N_\phi]$, the evolution equations for β_j are

$$\begin{pmatrix} \dot{\beta}_1 \\ \dot{\beta}_2 \\ \dot{\beta}_3 \end{pmatrix} = \mathbf{M}^{-1}\mathbf{D}\mathbf{M} \begin{pmatrix} \beta_1 \\ \beta_2 \\ \beta_3 \end{pmatrix} + \mathbf{M}^{-1} \begin{pmatrix} N_p \\ N_{u_\parallel} \\ N_\phi \end{pmatrix}, \tag{9}$$

where $\mathbf{D}$ is the matrix of the linear coupling, given by

$$\mathbf{D} = \begin{pmatrix} 0 & 0 & -i\omega_* \hat{\eta} \\ -ik_z & 0 & -ik_z \\ 0 & -\dfrac{ik_z}{1+k^2} & \dfrac{i\omega_*(\hat{\eta}k^2-1)}{1+k^2} \end{pmatrix}, \tag{10}$$

and N_p, $N_{u_\parallel}$, and N_ϕ are the nonlinearities defined in Eqs. (1)–(3). By construction, the matrix $\mathbf{M}^{-1}\mathbf{D}\mathbf{M}$ is diagonal, with elements $-i\omega_j$. Of greater significance is the form of the nonlinear terms. The three nonlinearities of the original representation are now mixed, so that linear combinations of all three enter each eigenmode evolution equation. Moreover, when the nonlinearities N_p, $N_{u_\parallel}$, and N_ϕ are written in terms of β_1, β_2, and β_3, each eigenmode is driven nonlinearly by every possible combination $\beta_m\beta_n$ with m and n each assuming values of 1–3. For example, the β_3 equation is

$$\dot{\beta}_3 + i\omega_3\beta_3 = \frac{(a_1-a_2)}{|\mathbf{M}|}N_p + \frac{(b_2-b_1)}{|\mathbf{M}|}N_{u_\parallel} + \frac{(a_2b_1-a_1b_2)}{|\mathbf{M}|}N_\phi, \tag{11}$$

where $|\mathbf{M}| = b_1a_2+b_2a_3+b_3a_1-b_3a_2-b_2a_1-b_1a_3$, and

$$N_p = -\sum_{k'} (\mathbf{k}' \times \hat{\mathbf{z}} \cdot \mathbf{k})(\beta_1' + \beta_2' + \beta_3') \times (b_1''\beta_1'' + b_2''\beta_2'' + b_3''\beta_3''), \tag{12}$$

$$N_{u_\parallel} = -\sum_{k'} (\mathbf{k}' \times \hat{\mathbf{z}} \cdot \mathbf{k})(\beta_1' + \beta_2' + \beta_3') \times (a_1''\beta_1'' + a_2''\beta_2'' + a_3''\beta_3''), \tag{13}$$

$$N_\phi = -\sum_{k'} (\mathbf{k}' \times \hat{\mathbf{z}} \cdot \mathbf{k})\frac{(k-k')^2}{(1+k^2)}(\beta_1' + \beta_2' + \beta_3') \times (\beta_1'' + \beta_2'' + \beta_3''). \tag{14}$$

We adopt the notational convention that when a_j, b_j, and β_j are unprimed, primed, or double-primed, it is understood that they depend on wave number k, k', or $k-k'$.

To examine the excitation of damped and marginally stable eigenmodes, consider the contribution made by the

interaction of β_1 with itself in the three nonlinear terms of Eq. (11). This portion of the right-hand side can be written

$$N_{311} = -\sum_{k'} (\mathbf{k}' \times \hat{\mathbf{z}} \cdot \mathbf{k}) \left[\frac{(a_1 - a_2)}{|\mathbf{M}|} b_1'' + \frac{(b_2 - b_1)}{|\mathbf{M}|} a_1'' + \frac{(a_2 b_1 - a_1 b_2)}{|\mathbf{M}|} \frac{(k-k')^2}{(1+k^2)} \right] \beta_1' \beta_1''. \tag{15}$$

This component of the β_3 nonlinearity is vital to β_3 evolution because, provided the system starts from infinitesimal amplitude in all eigenmodes, it causes β_3 to grow exponentially. Under linear theory the eigenmode is damped. The growth process is parametric instability, where the exponential growth of unstable β_1 modes at k' and $k-k'$ makes N_{311} grow exponentially, imposing an exponentially growing force to β_3. Until β_3 becomes large enough to act back on β_1 in a significant way, N_{311} acts as an external force. It drives exponential growth independent of the complex β_3 amplitude, and does so until β_1 saturates. Modes on the β_1 branch that are damped do not prevent the growth; their contribution to N_{311} merely decays so that N_{311} is governed by wave numbers for which $\beta_1' \beta_1''$ is growing. Although the summation in N_{311} ranges over positive and negative values of k', the summand for $k' > 0$ does not cancel the summand for $k' < 0$, because $\beta_1(-k') = \beta_1^*(k')$, and the $k-k'$ dependence breaks symmetry. A term like N_{311} operates in like fashion in every damped and marginally stable eigenmode.

Parametric instability is well known. Here it applies to every stable eigenmode in the basis set, provided the coefficients in the forcing terms [e.g., Eq. (15)] are not all zero. No stable eigenmode decays to zero, rather all experience exponential growth to a level determined by saturation balances. This assertion is quite general, hence we provide further explanation and essential qualifications. The following are written as general statements, but are illustrated mathematically using the ion model.

1. Parametric growth occurs provided initial amplitudes are sufficiently small to make all nonlinear terms much smaller than the linear terms initially. This guarantees that all damped eigenmodes initially decay at the linear damping rate, and marginal modes remain constant (after a transient that sets up the eigenmode phases).
2. While damped eigenmodes are decaying from initial values, terms like N_{311} are growing exponentially. Because of 1 above, some time elapses before the exponential growth of terms like N_{311} overtakes the decay from the initial level. If there are multiple eigenmode branches with unstable modes, each contributes a term like N_{311} to the evolution of the damped β_3 eigenmode. However, the beating of modes on the fastest growing branch will dominate the parametric drives from other unstable branches. Nonlinear terms in which a growing mode beats with a damped or marginal mode, or damped or marginal modes beat with each other, are smaller than terms in which two growing modes interact. This is because growing modes increase exponentially from their initial value, whereas damped modes decrease exponentially until terms like N_{311} have grown sufficiently to exceed linear terms.
3. The evolution of β_3 under parametric instability is obtained by solving

$$\dot{\beta}_3 = -i\omega_3 \beta_3 + \sum_{k'} \hat{N}_{311} \exp[-i(\omega_1' + \omega_1'')t], \tag{16}$$

where unprimed, primed, and double-primed quantities indicate dependence on wave numbers k, k', and $k-k'$, and

$$\hat{N}_{311} = -(\mathbf{k}' \times \hat{\mathbf{z}} \cdot \mathbf{k}) \left[\frac{(a_1 - a_2)}{|\mathbf{M}|} b_1'' + \frac{(b_2 - b_1)}{|\mathbf{M}|} a_1'' + \frac{(a_2 b_1 - a_1 b_2)}{|\mathbf{M}|} \frac{(k-k')^2}{(1+k^2)} \right] \beta_{10}' \beta_{10}''. \tag{17}$$

In writing Eqs. (16) and (17), $\beta_1(k,t)$ is approximated by its linear evolution, $\beta_1(k,t) = \beta_{10} \exp[-i\omega_1 t]$, consistent with 1 and 2 above. The solution of Eq. (16) is

$$\beta_3 = \sum_{k'} \frac{\hat{N}_{311}\{\exp[-i(\omega_1' + \omega_1'')t] - \exp[-i\omega_3 t]\}}{-i(\omega_1' + \omega_1'' - \omega_3)} + \beta_{30} \exp[-i\omega_3 t]. \tag{18}$$

For $t < (\omega_1' + \omega_1'')^{-1}$, ω_3^{-1}, the first term grows linearly in time from zero value ($\beta_3 \sim t$). Once $t \approx \omega_3^{-1}$, it grows exponentially from an amplitude $\sim \hat{N}_{311}/(\omega_1' + \omega_1'' - \omega_3)$. The second term describes the decay from the initial level. Under 1,

$$\omega_3 \beta_{30} \gg \sum_{k'} \hat{N}_{311}. \tag{19}$$

This guarantees that the decaying second term dominates the evolution initially.
4. The first term of Eq. (18) overtakes the decaying second term before the saturation of β_1 or β_3, i.e., while the parametric instability approximation remains valid. This follows because saturation of β_1 requires that nonlinear terms become larger than the linear term of the β_1 equation, $-i\omega_1\beta_1$, which is growing exponentially in time. The first term of Eq. (18) overtakes the second term when a nonlinear term becomes larger than a linear term which is *decaying* exponentially.
5. The parametric instability approximations that make Eqs. (16)–(18) valid remain in force until either β_1 saturates (a nonlinear term balances $-i\omega_1\beta_1$), or until another nonlinear term in the β_3 equation becomes as large as N_{311}.
6. The entire system saturates when nonlinearities in the unstable eigenmode equations become as large as the linear drive terms, because the latter supply instability free energy. It is possible that nonlinear terms involving stable eigenmodes are smaller than those involving growing eigenmodes. In this case the stable eigenmodes, although subject to nonlinear, exponential growth, do not reach a sufficient level to affect saturation significantly, and can be ignored in analyses of saturation and calculations of growth rates and transport fluxes.

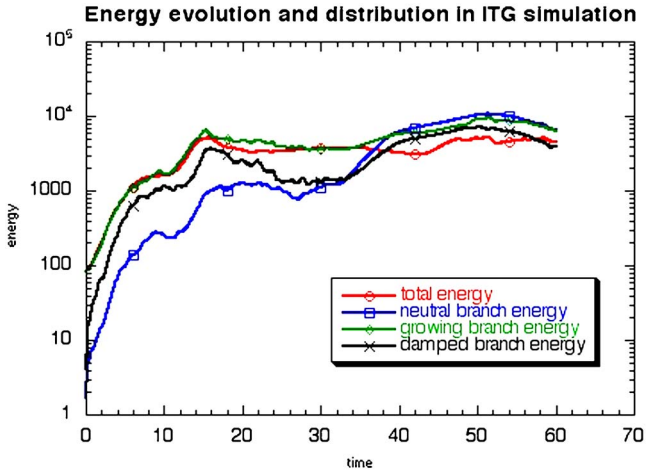

FIG. 2. Time evolution of the total energy, and the energy associated with squared eigenmode amplitudes β_1^2, β_2^2, and β_3^2.

Damped eigenmodes cannot be ignored if any nonlinear term involving a damped eigenmode becomes large enough to affect a saturation balance.

Numerical solutions of Eqs. (1)–(3) show that both the damped and marginally stable eigenmodes are important in saturation. One indication is the evolution of the fluctuation energy,

$$U = \sum_k U_k = \sum_k [(1+k^2)|\phi|^2 + |u_\parallel|^2 + |p|^2]. \tag{20}$$

We express U in terms of the eigenmode amplitudes β_m using Eq. (8),

$$U = \sum_k \left\{ \sum_{m=1}^{3} [(1+k^2)|a_m|^2 + |b_m|^2 + |c_m|^2]|\beta_m|^2 + 2\,\mathrm{Re} \sum_{m=1}^{2} \sum_{n>m}^{3} [(1+k^2)(a_m a_n^*) + (b_m b_n^*) + (c_m c_n^*)] \times \langle \beta_m \beta_n^* \rangle \right\}. \tag{21}$$

Figure 2 shows the time evolution of the total fluctuation energy and the three autocorrelation terms (proportional to $|\beta_m|^2$) of Eq. (21), generated from a numerical solution. Exponential growth is clearly evident. In the last phase of evolution, the sum of the autocorrelation terms exceeds $3U$. Consequently, the sum of the cross-correlation terms (proportional to $\langle \beta_m \beta_n^* \rangle$) is negative and its magnitude exceeds $2U$. Virtually all terms of Eq. (21) appear to make a significant contribution to U.

Before showing the results of that comparison, it is useful to develop a criterion that identifies when stable eigenmodes affect saturation. Our criterion uses only model parameters, i.e., linear and nonlinear coupling coefficients, allowing simple inspection to determine if stable eigenmodes are important. The criterion also provides insight into how damped eigenmodes break the hegemony of unstable eigenmodes. The criterion is heuristic and generic, but will be tested against solutions of the ion and CTEM models.

Consider two eigenmodes x_1 and x_2 whose dominant coupling can be represented by

$$\dot{x}_1 = \gamma_1 x_1 + C_1 x_1^2 + D_1 x_1 x_2, \tag{22}$$

$$\dot{x}_2 = -\gamma_2 x_2 + C_2 x_1^2 + \ldots . \tag{23}$$

We assume that $\gamma_1 > 0$ and $\gamma_2 \geqslant 0$. This makes x_1 linearly unstable and x_2 linearly damped or marginally stable. The term $C_2 x_1^2$ drives parametric instability in the stable eigenmode. These need not be the only two eigenmodes in the system or the only couplings, but they are the couplings that describe how a parametrically unstable eigenmode that is linearly stable most directly feeds back on an unstable eigenmode. If there are other eigenmodes, x_2 is the eigenmode that is most strongly driven by the parametric process, i.e., C_2 is larger than the parametric coupling in the equations for the other eigenmodes. The term $C_1 x_1^2$ is normally assumed to saturate the instability when stable eigenmodes are ignored. In this simple representation we are not tracking a spectrum of Fourier modes. The unstable eigenmode first grows linearly according to

$$x_1 = x_i \exp[\gamma_1 t], \tag{24}$$

where x_i is an initial amplitude. The second eigenmode experiences the combination of initial decay and parametric growth described previously, and evolves according to

$$x_2 = \frac{C_2 x_i^2}{\gamma_2 + 2\gamma_1}[\exp(2\gamma_1 t) - \exp(-\gamma_2 t)] + x_i \exp(-\gamma_2 t), \tag{25}$$

where for simplicity we have assumed that x_2 has the same initial value as x_1.

We now consider the threshold under which x_2 affects saturation. This is a requirement imposed on the first equation, because that is where the instability resides. The stable eigenmode affects saturation when

$$D_1 x_1 x_2 \approx C_1 x_1^2. \tag{26}$$

When Eqs. (24) and (25) are substituted into this expression to yield

$$\frac{D_1 C_2 x_i^2}{(\gamma_2 + 2\gamma_1)} \exp(2\gamma_1 t) \approx C_1 x_i \exp(\gamma_1 t), \tag{27}$$

it represents the condition under which a stable eigenmode reaches a sufficient level via parametric excitation to affect saturation. In making the substitution we retain only the exponentially growing part of Eq. (25). The condition now depends on time. We are interested in the time at saturation, which we define as the time required for the exponential linear growth of Eq. (22) to bring the standard nonlinear term $C_1 x_1^2$ up to the level of the linear term. Therefore, at saturation $\gamma_1 \approx C_1 x_i \exp(\gamma_1 t)$, allowing time to be eliminated in the threshold condition. The condition expressed in Eq. (26) for the threshold of stable eigenmode effects in saturation then becomes

TABLE I. Summary of couplings in ion model, grouped according to interactions between a mode on the growing eigenmode branch and a second mode on the growing, damped, or neutral branch. The values of N_{ijm} should be multiplied by 10^{-3}.

Wave number				Growing	Damped				Neutral		
				C_1	C_2	D_1		C_2	D_1		
k_x	k_y	k'_x	k'_y	$\lvert N_{111}\rvert$	$\lvert N_{311}\rvert$	$\lvert N_{113}\rvert$	$\lvert N_{131}\rvert$	$\lvert N_{211}\rvert$	$\lvert N_{112}\rvert$	$\lvert N_{121}\rvert$	P_t
0.1	0.1	−0.2	0.2	3.8	1.5	1.2	3.5	2.4	1.4	4.3	0.35
0.3	0.4	0.4	0.3	54	61	74	80	1.2	30	76	0.56
0.5	0.6	−0.2	0.2	46	12	46	123	6.1	12	34	0.23

$$P_t \equiv \frac{D_1 C_2}{C_1^2(2+\gamma_2/\gamma_1)} \approx 1. \tag{28}$$

This condition depends only on nonlinear coupling coefficients and growth rates, with the latter deriving from linear coupling coefficients. However, the nonlinear coupling is between modes on distinct branches of the dispersion relation, hence the nonlinear coefficients also depend on the linear coupling coefficients through the eigenmode decomposition matrix **M**. Initial levels do not enter because they were assumed equal for all eigenmodes.

According to Eq. (28), the couplings that drive the damped eigenmode parametrically, and allow it to affect the growing eigenmode, must be competitive with the coupling of Kolmogorov-like spectral transfer on the growing branch (given by $C_1 x_1^2$). The competition is one of straightforward ratios. If the parametric drive is weaker than the Kolmogorov transfer, $C_2/C_1 < 1$, the coupling of the damped branch in the evolution of the unstable eigenmode must be that much stronger, i.e., $D_2/C_1 \approx C_1/C_2 > 1$. However, there is also an important dependence on growth and damping rates. This factor parametrizes the ratio of nonlinear interaction time to the time required to achieve saturation. If the damped eigenmode is heavily damped relative to the growth of the unstable eigenmode, $\gamma_2/\gamma_1 \gg 1$, the couplings of the damped branch must become significantly stronger ($C_2 D_1/C_1^2 \gg 1$) for it to have an effect. Greatly increasing the damping rate of a damped branch does not negate its exponential growth or change the rate of exponential growth. Instead, as is clear from Eq. (25), it gives it such a small amplitude factor that it becomes difficult for it to compete with Kolmogorov transfer on the time scale of saturation. Note that the damping rate only becomes a significant factor once it exceeds the instability growth rate. An eigenmode with $\gamma_2 \approx \gamma_1$ is essentially at no disadvantage relative to an eigenmode with $\gamma_2 \approx 0$. This is an important observation. With $\gamma_2 \approx \gamma_1$ there is a potent energy sink for saturation, yet the damping is not too large to prevent parity in energy balances, provided the coupling factors are favorable. This typifies both CTEM and the ion model. Moreover, it implies that zonal modes of a damped eigenmode can have a greater impact than conventional zonal modes (marginally stable or weakly damped). This too is observed in CTEM.

As far as couplings go, the threshold condition of Eq. (28) is intuitively reasonable. However, the couplings are nontrivial because they apply to generally ignored stable eigenmodes. An example of C_2 for the ion model is N_{311} [Eq. (15)]. The expression for C_1 and D_1 are similarly complex. All depend on eigenvector components. Given this complexity it is worth checking that Eq. (28) properly describes systems where stable eigenmodes play a significant role in saturation and those where they do not. For CTEM turbulence,[19,23,24] $\gamma_2/\gamma_1 \approx 1$, $C_2/C_1 \approx 1$, and $D_1/C_1 \approx \delta^{-2} \gg 1$, where δ is the small ratio of collision frequency to diamagnetic frequency. Thus $P_t = C_2 D_1/C_1^2(2+\gamma_2/\gamma_1) = O(\delta^{-2}) \gg 1$, indicating that the damped branch does not merely become as important as the growing branch in saturation, but that it *dominates* saturation, rendering the Kolmogorov saturation channel unimportant.[24] This prediction is observed in simulations, and verified by solving for the saturation level in a detailed statistical closure theory. The CTEM model also holds in the collisional limit. There $C_2/C_1 \approx 1$, while $D_1/C_1 \approx \delta$, where $\delta \gg 1$ in the collisional limit. However, the normalized damping rate is larger, of order δ^2. Consequently $P_t = O(\delta^{-1}) \ll 1$, and the damped branch is not predicted to play a role in saturation. This also was verified in simulations of the 2-field trapped electron mode system.[19] Note that in the collisional case the damped branch coupling is potent, but the parametric growth cannot reach a sufficiently high level because of the strong damping. It is also worth pointing out that C_1 and C_2 are coefficients of a coupling product, $\beta_1(k')\beta_1(k-k')$, that is symmetric under the exchange $k' \leftrightarrow (k-k')$. If the leading order of C_1 and C_2 are constant, this order vanishes in the sum over k', and the next higher order (which will depend on k' or $1/k'$) must be used in Eq. (28). This occurs in the CTEM model, effectively increasing D_1/C_1.

The complexity of the coupling coefficients in the ion model makes it difficult to evaluate Eq. (28) by inspection. Accordingly, we have evaluated the coupling coefficients numerically for several wave numbers and have summarized the results in Table I. The table gives the values of N_{ijm} for values of i, j, and m that represent the parametric driving of damped and neutral modes (N_{311} and N_{211}), the forcing of damped and neutral modes on the growing mode (N_{113}, N_{131}, N_{112}, and N_{121}), and the Kolmogorov transfer involving interactions of modes solely on the growing branch (N_{111}). These three classes of interactions are represented in the heuristic model by C_2, D_1, and C_1, respectively. The table also gives the largest value estimated for the threshold parameter P_t, given by the right-hand side of Eq. (28). The wave num-

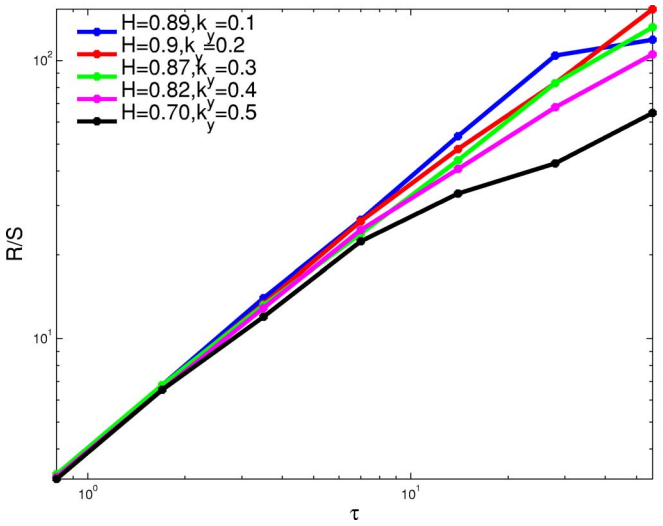

FIG. 3. Hurst exponents for Fourier modes with $k_x=0$ and $k_y=0.1$, 0.2, 0.3, 0.4, and 0.5.

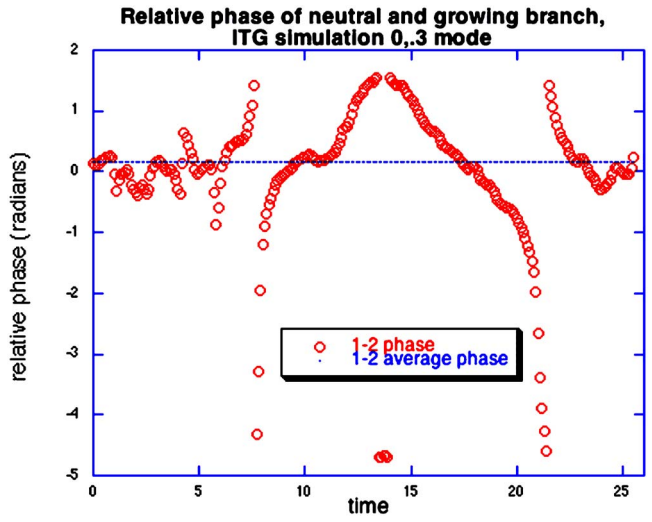

FIG. 4. Time evolution of the phase of $\langle \beta_1(k)\beta_2^*(k)\rangle$ for the mode $k_x=0$, $k_y=0.3$.

bers correspond to cases in which the neutral mode plays a slightly larger role in saturation than the damped mode ($k_x=0.1$, $k_y=0.1$), the damped mode plays the larger role ($k_x=0.3$, $k_y=0.4$), and a case in which the growth rate of the parametric drive is weak ($k_x=0.5$, $k_y=0.6$). The results indicate that both damped and neutral eigenmodes play a comparable and significant role in saturation, but that neither achieves the hegemony of the damped eigenmode in CTEM turbulence.

This assessment is borne out by simulation results, the most striking feature of which is a robust, intrinsic temporal intermittency in all measured quantities. The intermittency is evident in standard measures, including the probability distribution function (PDF) and the Hurst exponent.[26] Figure 3 shows Hurst exponents for Fourier modes with $k_x=0$ and various k_y values. The exponent lies between 0.7 and 0.9 in all cases, indicating persistent long time correlations on scales of at least 60 time steps. For reference, the nonlinear decorrelation (eddy turnover) time of the $k_y=0.3$ mode is of order 2 time steps, as inferred from the discussion of Fig. 4 below. Hurst exponents around 0.5 are the norm for Gaussian correlations. Enhanced values in the range of 0.7 and above have been linked to system-scale correlations mediated by global avalanche-like transport events in systems with relaxing gradients and self-organized criticality.[27] Here the driving gradient is rigidly fixed. Figure 3 indicates a trend toward less intermittent behavior with increasing wave number. This is consistent with transition at high k from the wave-dominated regime, and a corresponding diminution of the importance of wave eigenmode properties. However, the long time-scale correlations of the modes in Fig. 3 dominate in spectrum averaged quantities such as energies and transport fluxes. Figure 5 shows the PDF of $\Sigma k_y b_1 |\phi_k|^2$, which is a weighted energy proportional to the quasilinear heat flux. There is a distinct deviation from a Gaussian in the tail. This is produced by the long time correlations detected through the Hurst exponent in Fig. 3.

Two features of time histories that relate to the intermittency are worth discussing. First, fluctuations radically change character at random intervals longer than a nonlinear correlation time. Second, growth rates, transport fluxes, and quantities tied to the free-energy source, which is destabilizing and rigidly fixed, intermittently transition from positive to negative values. Neither behavior was observed in CTEM turbulence, which nonetheless had nontrivial cross-correlation dynamics. Both are consistent with a situation in which multiple eigenmode branches compete for hegemony on a nearly equal footing in the energy balances of saturation, as suggested by Table I. An example of the first behavior is the evolution of the phase of cross correlations between eigenmodes. Figure 4 shows the evolution of the phase of $\langle \beta_1(k)\beta_2^*(k)\rangle$. During certain times, i.e., for $0<t<7$ and t

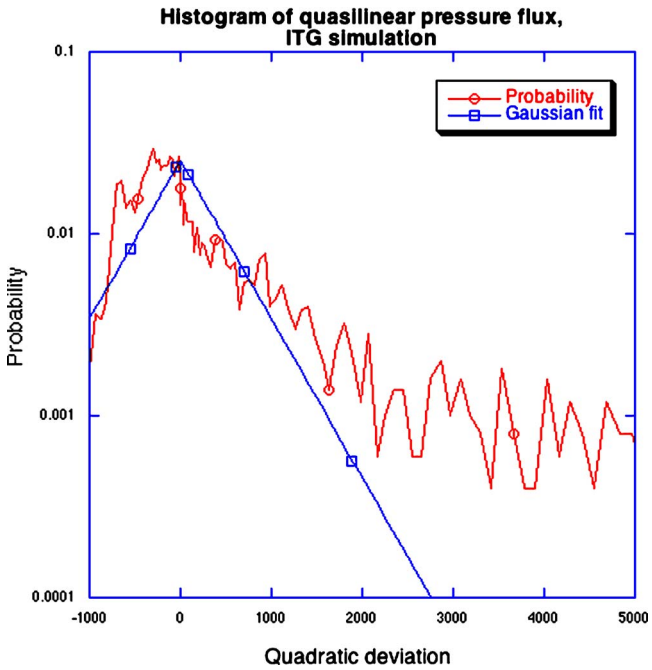

FIG. 5. Probability distribution function for $\Sigma k_y b_1 |\phi_k|^2$ constructed from the time history. The least-squares-fitted Gaussian is plotted as a benchmark.

>22, the phase appears locked to zero in an average sense. The rms value of random fluctuations about the mean is 0.5 radians, and their time scale is a nonlinear decorrelation (eddy turnover) time. For $7<t<9$ and $20<t<22$ the phase evolution is radically different with rotation at a roughly constant rate through the angle 2π. In between the periods of rapid rotation, the rotation slows and changes sign, but does not show evidence of incoherence. The eigenmode cross correlation in CTEM turbulence evinces only locked behavior. There the mean angle is zero, consistent with a simple representation of the damped eigenmode as an oscillator driven continuously by the sinusoidal external forcing of two coupled unstable eigenmodes. The rms amplitude of incoherent fluctuations about the mean does not exceed 0.3 radians.

Examples of growth rates and fluxes showing the second type of behavior will be given in the next section. The temporal intermittency of the ion model, and its absence in CTEM turbulence, seems to be consistent with the near unity values of P_t for all eigenmodes in the former, and the large value of P_t in the latter.

IV. INSTABILITY DRIVE AND TRANSPORT

When mode coupling terms involving stable eigenmodes enter saturation balances on a par with terms involving only the unstable eigenmode, it is likely that the growth rate is significantly modified. This follows from the simple observation that the growth rate and the nonlinearities that govern saturation all depend on quadratic correlations of the fluctuating fields. To formulate the growth rate as a general property of the system, not just of the linearly unstable eigenmode, it is derived from the time derivative of the fluctuation energy. The time derivative captures dissipation, including the dissipation by which energy is introduced into the turbulence from the driving gradients, and removed, for example, by collisional processes. For conservative nonlinearities like N_p, $N_{u_\parallel}$, and N_ϕ, spectral energy transfer rates drop out of the derivative when energy is properly formulated. The derivative therefore constitutes a generalized growth rate, valid at both infinitesimal and finite amplitude. Returning to Eq. (20) for the fluctuation energy, we take the time derivative to obtain

$$\frac{\partial U}{\partial t} = \sum_k [k_z \,\mathrm{Im}\langle p u_\parallel^* \rangle + v_D k_y \hat{\eta}_e \,\mathrm{Im}\langle \phi p^* \rangle - \gamma_D U_k], \tag{29}$$

where γ_D is the net dissipation of viscosities and collisional diffusivities that are included for numerical simulation.

The net input rate of energy at each wave number, exclusive of conserved spectral energy transfer, is the summand of this expression divided by the energy U_k, and is labeled γ_k^{nl}:

$$\gamma_k^{\mathrm{nl}} = \frac{k_z \,\mathrm{Im}\langle p u_\parallel^* \rangle + k_y \hat{\eta}_e \,\mathrm{Im}\langle \phi p^* \rangle}{U_k} - \gamma_D. \tag{30}$$

The first term of the numerator represents free energy released to ion acoustic motion through parallel compressibility. The second term represents the free energy of the ion temperature gradient released through $E\times B$ advection of the gradient. The second term tends to dominate for linearly unstable modes and typical wave numbers. This term depends on the same coupling of fields as in the nonlinearity N_p, hence it introduces into γ_k^{nl} terms that correspond to couplings in each saturation equation. Writing Eq. (30) in terms of the eigenmode amplitudes,

$$\begin{aligned}\gamma_k^{\mathrm{nl}} = \{\mathrm{Im}[&|\beta_1|^2[b_1 a_1^* k_z + b_1^* k_y \hat{\eta}_e] + |\beta_2|^2[b_2 a_2^* k_z + b_2^* k_y \hat{\eta}_e] + |\beta_3|^2[b_3 a_3^* k_z + b_3^* k_y \hat{\eta}_e] + \langle \beta_1 \beta_2^* \rangle (b_1 a_2^* k_z + b_2^* k_y \hat{\eta}_e) + \langle \beta_1^* \beta_2 \rangle (a_1^* b_2 k_z \\ &+ b_1^* k_y \hat{\eta}_e) + \langle \beta_1 \beta_3^* \rangle (b_1 a_3^* k_z + b_3^* k_y \hat{\eta}_e) + \langle \beta_1^* \beta_3 \rangle (a_1^* b_3 k_z + b_1^* k_y \hat{\eta}_e) \\ &+ \langle \beta_2 \beta_3^* \rangle (b_2 a_3^* k_z + b_3^* k_y \hat{\eta}_e) + \langle \beta_2^* \beta_3 \rangle (a_2^* b_3 k_z + b_2^* k_y \hat{\eta}_e)]\} U_k^{-1} - \gamma_D,\end{aligned} \tag{31}$$

the growth rate is revealed as potentially far more complicated than Eq. (30) suggests. This complexity vanishes if the unstable eigenmode is the only eigenmode of consequence, i.e., $\beta_2 \to \beta_3 \to 0$. Then Eq. (31) becomes

$$\gamma_k^{\mathrm{nl}} \to \frac{|\beta_1|^2 \,\mathrm{Im}[b_1 a_1^* k_z + b_1^* k_y \hat{\eta}_e]}{U_k|_{\beta_2=\beta_3=0}} - \gamma_D \equiv \gamma_k^{\mathrm{linear}}, \tag{32}$$

and the linear growth rate is recovered. However, the four terms $k_y \hat{\eta}_e \,\mathrm{Im}[b_2^* \langle \beta_1 \beta_2^* \rangle + b_1^* \langle \beta_1^* \beta_2 \rangle + b_3^* \langle \beta_1 \beta_3^* \rangle + b_1^* \langle \beta_1^* \beta_3 \rangle]$ are part of D_1 in the heuristic model, and $\mathrm{Im}\, b_1^* k_y \hat{\eta}_e |\beta_1|^2$ is part of C_1. The values of P_t in Table I indicate that these terms all contribute significantly to the growth rate. The values of P_t also indicate that all three eigenmodes broker saturation, from which it is reasonable to conclude that all nine terms of γ_k^{nl} contribute in a meaningful way. Clearly, there are hidden degrees of freedom (i.e., sources of variability) not evident in the simple expression of Eq. (30).

This view is further supported by Fig. 6, which shows the time history of γ_k^{nl} for a linearly unstable wave number. This quantity is extremely oscillatory, with fluctuations that are much larger than the mean and cause the growth rate to alternate from positive to negative values. The time average, computed over the full time domain of the plot, is indicated by the smaller of two constants. The linear growth rate for this wave number is larger and also shown. The time domain is very long compared to that of Fig. 4, so that the time scale of variation evident in the figure is 20 time units or more. Recall that the nonlinear correlation time (eddy turnover time), identified as the time scale of fluctuations about the

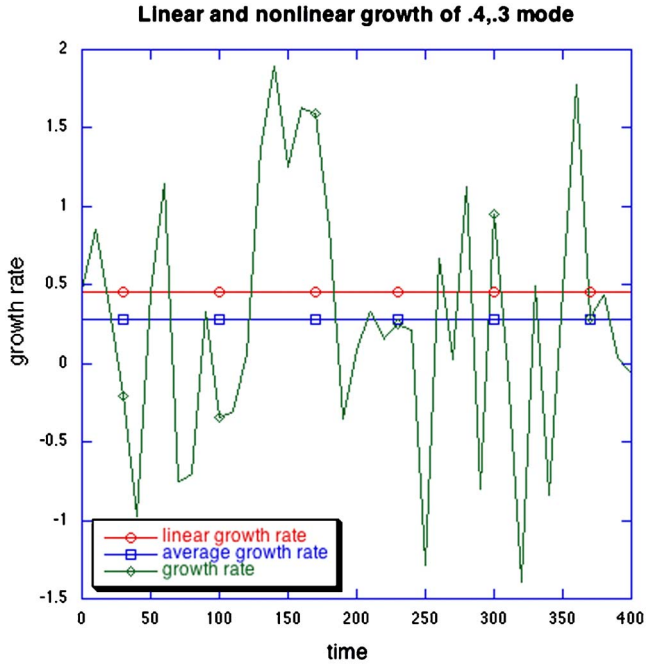

FIG. 6. Time evolution of γ_k^{nl} for $k_x=0.3$, $k_y=0.4$. Also plotted are the time average of γ_k^{nl} over the entire domain, and the linear growth rate.

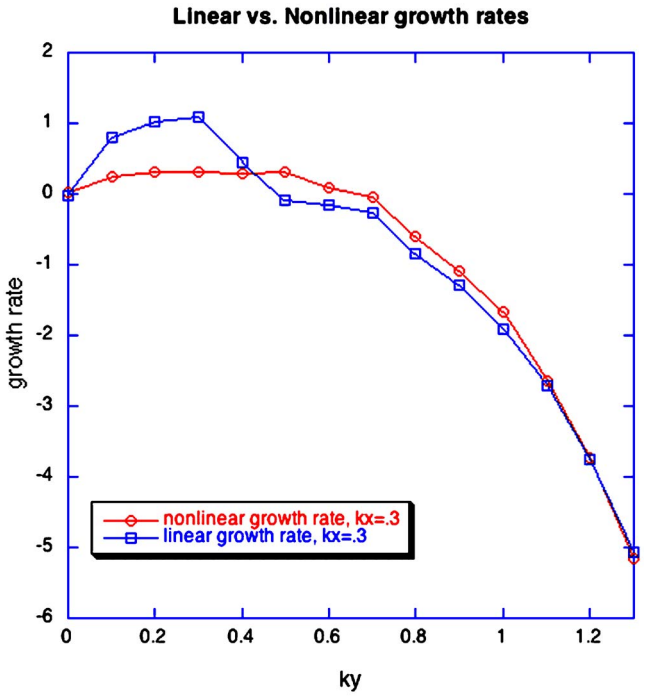

FIG. 7. Long-time averaged growth rate spectrum in k_y for $k_x=0.3$, showing γ_k^{nl} and $\gamma_k^{\mathrm{linear}}$.

mean phase in the locked regime of Fig. 4, is approximately two time units. Hence, the fluctuations in Fig. 6 represent events with persistent correlations, on the order of 10 nonlinear decorrelation times or more.

To better appreciate the variability evident in this plot, we observe that growth rates in fixed gradient turbulence are generally assumed to be constant. The reason is simple: in $\gamma_k^{\mathrm{linear}}$, as obtained from Eq. (31) or (32) by setting $\beta_2=\beta_3=0$, the numerator and the denominator U_k are each proportional to $|\beta_1|^2$. This factor cancels out to yield an expression that is independent of amplitude. As such, it depends only on constants, provided the driving gradients remain fixed. Allowing for nonlinear effects, the derivation of $\gamma_k^{\mathrm{linear}}$ from γ_k^{nl} shows that γ_k^{nl} remains constant if any one eigenmode dominates Eq. (31). Moreover, even with all eigenmodes present, and accounting for fluctuations about mean values, if the cross correlations are phase locked (stationary), and all correlations have fluctuations whose rms value is like those of the locked phase in Fig. 4, the growth rate should be stationary with small fluctuations that vary on the nonlinear correlation time scale. The extreme variability of Fig. 6 requires cross correlations whose phases are not locked, and that enter the dominant coterie of the growth rate expression. It is not surprising that the largest time scale of the growth rate variation is the time scale over which cross phases remain locked or unlocked. The growth rate variability is likely facilitated by the transitional values of P_t in Table I. All eigenmodes compete, but none dominate, precluding phase locking for indefinite time periods.

Another feature of Fig. 6 is the reduced value of the average growth rate relative to the linear growth rate, representing a suppression of the linear instability for this wave number. If there is phase locking, it is possible for the cross correlations to be large and positive and thereby increase the linear growth rate, as occurs for $120<t<180$. It is also possible for the cross correlations to be large and negative as occurs transiently at various times, thereby decreasing the growth rate by more than the damping rate of the damped eigenmode. However, if locked phases with these properties cannot persist, the cross-correlation contributions to the growth rate can be expected to phase average to zero over a long time. If this happens, the only terms contributing to the growth rate for long time averages are the first three terms of Eq. (31). The first represents the growth of the unstable mode and is positive for all times if the wave number is in the unstable range. The second represents the marginal mode and is close to zero. The third represents the damped mode and is negative. With the damped eigenmode excited, its negative contribution to Eq. (31) lowers the growth rate, as observed.

The reduction of linear growth rate is actually considerably more pronounced in modes that are more unstable. Figure 7 shows the variation of γ_k^{nl} with k_y for k_x fixed, averaged over the entire time domain of Fig. 6. The linear growth rate is also plotted. The value of γ_k^{nl} for wave numbers throughout the unstable range is approximately constant while the most unstable modes have linear growth rates that are three times as large. (For the mode described in Fig. 6 the wave number is close to the instability boundary and its smaller linear growth rate is not so much larger than γ_k^{nl}). For wave numbers just beyond the unstable range, there is weak nonlinear instability. This occurs because the cross correlations are positive and larger than the first three terms of Eq. (31) on average. Calculation of the growth rate for $k_x=0$ shows that for k_y in the lowest wave-number part of the unstable range, γ_k^{nl} is essentially unchanged from $\gamma_k^{\mathrm{linear}}$.

The correlations of growth rate and transport are closely related. The time-averaged reduction of the growth rate by

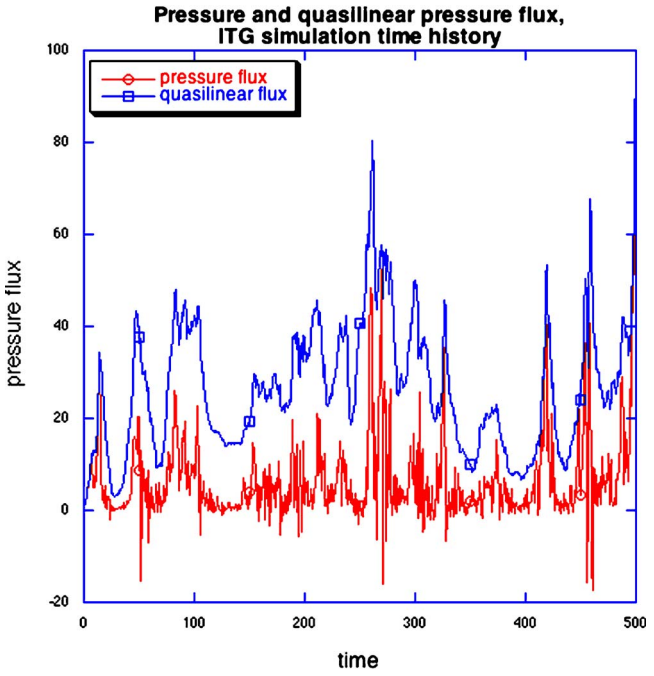

FIG. 8. Time evolution of the quasilinear heat flux and true heat flux for long times. The true flux is both smaller and more bursty. Driving gradients are fixed.

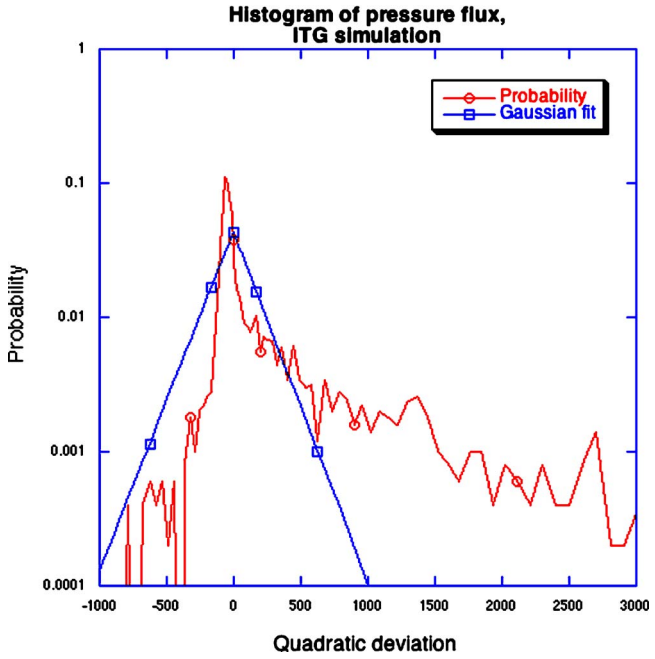

FIG. 9. Probability distribution of the heat flux. The non-Gaussian tail is more pronounced than it is in the quasilinear flux, as explained in the text. The least-squares-fitted Gaussian is plotted as a benchmark.

the damped eigenmode should also reduce transport fluxes. The ion model allows transport of parallel momentum and heat. We consider the thermal flux given by

$$Q = \sum_k k_y \,\mathrm{Im}\langle \phi^* p \rangle. \tag{33}$$

This flux is evaluated from the numerical solutions for p and ϕ^* at each wave number. The quasilinear flux is obtained in a similar way except that instead of taking the actual field amplitude for p, the eigenvector of the linearly unstable eigenmode, $b_1\phi$, is used and $|\phi|^2$ is taken from numerical solutions. Time histories of the true flux and quasilinear flux are compared in Fig. 8. The true flux follows the quasilinear flux initially while amplitudes remain below the threshold for nonlinear effects. After saturation the true flux is strongly reduced and shows bursty behavior, despite fixed gradients. Between bursts the flux is nearly zero. During bursts it is reduced by a factor of 2 to 4, but also has brief negative transients.

The PDF of the flux is shown in Fig. 9. The stronger tail enhancement relative to the quasilinear flux indicates that long time correlations in individual modes at low wave number, as depicted in Fig. 3, have a disproportionately larger effect on the flux cross correlation $\langle \phi^* p \rangle$ than on the autocorrelation $b_1|\phi|^2$. This can be understood from the expression of the flux in terms of the eigenmode amplitudes,

$$\begin{aligned} Q = \sum_k k_y \hat{\eta}_e \,\mathrm{Im}\{ & |\beta_1|^2 b_1^* + |\beta_2|^2 b_2^* + |\beta_3|^2 b_3^* \\ & + \langle \beta_1 \beta_2^* \rangle b_2^* + \langle \beta_1^* \beta_2 \rangle b_1^* \\ & + \langle \beta_1 \beta_3^* \rangle b_3^* + \langle \beta_1^* \beta_3 \rangle b_1^* + \langle \beta_2 \beta_3^* \rangle b_3^* + \langle \beta_2^* \beta_3 \rangle b_2^* \}. \end{aligned} \tag{34}$$

The flux bursts have a duration of tens of nonlinear correlation times, and are thus tied to locking and unlocking of cross phases, just as the growth rate variability. Phase rotation mixes the contribution of cross correlations in Eq. (34). The remaining autocorrelation terms can also cancel, depending on amplitudes, because b_2^* and b_3^* are negative whereas b_1^* is positive. The quasilinear flux, on the other hand, is positive definite. Its cross-correlation terms also phase mix but its autocorrelation terms are positive definite. As a result, the quasilinear flux is larger and has a positive value when mixing is strong. The exact flux tends to be near zero when mixing is strong, accentuating the bursts that occur with locking and enhancing the contribution of long time correlations. This description is simplified and the dynamics merits further scrutiny, not in the least because the variability here attributed to phased interactions between eigenmodes bears a striking superficial resemblance to variability found in systems with evolving near-critical profiles and nonlocally correlated transport.[27] Profile relaxation and nonlocal effects are not present here and play no role in the dynamics. We anticipate that part of the difference between the quasilinear and true flux scales independently of L_T, and therefore represents a nonlinear heat pinch.[22]

V. CONCLUSIONS

We have undertaken a consideration of the role of stable eigenmodes in the saturation, instability, and transport in systems for local, quasihomogeneous drift turbulence described by multiple fields. From a heuristic description of parametric excitation and the nonlinear coupling between eigenmodes, we have developed a threshold condition indicating when stable eigenmodes can cause significant changes in saturation dynamics. We have applied this condition to prior results from collisionless and dissipative trapped electron turbu-

lence, and to new results from a simple 3-field model for ion turbulence driven by ion temperature gradient.

We conclude that stable eigenmodes are always nonlinearly destabilized through parametric excitation arising from the beating of two coupled modes on the unstable eigenmode branch. Initial levels must be sufficiently low to yield a regime of linear growth. The growth rate of parametric excitation is exponential, with an amplitude governed by the inverse of the additive sum of unstable eigenmode growth rates and stable eigenmode damping rate. If time to saturation is factored out, the amplitude factor depends on the ratio of damping rate to growth rate. As long as the damping is no larger than the growth, this factor does not strongly affect stable eigenmodes. If the damping is stronger, the stable eigenmode may not affect saturation. The question of whether stable eigenmodes affect saturation is also one of coupling strengths The coupling of interacting unstable eigenmodes to stable branches, and the feedback of nonlinearly excited stable eigenmodes on the evolution of the unstable eigenmode, must be large enough to maintain parity with Kolmogorov-like spectral transfer. The correlations that determine nonlinear coupling also govern the extraction of instability free energy and transport fluxes, although the relationship is not one-to-one. It is likely that if stable eigenmodes affect saturation they will also affect the instability drive and transport.

The nonlinear couplings involving stable eigenmodes are directly related to the structure of eigenvectors forming a complete basis set. For CTEM turbulence this coupling is very strong and the stable eigenmode dominates the saturation dynamics. In the collisional limit this coupling is weakened somewhat but remains stronger than Kolmogorov transfer. However, the stable eigenmode damping rate is very large compared to the instability growth rate, and the stable eigenmode is unable to achieve a sufficient level to affect the turbulence. This dichotomy of behavior is captured in a parametrization of the threshold condition via a threshold parameter P_t. For CTEM turbulence $P_t \gg 1$, while for the collisional limit $P_t \ll 1$. For the ion model $P_t \lesssim 1$ for all stable eigenmodes. These transitional values of P_t are associated with the following:

1. The damped and marginally stable eigenmodes are excited to significant levels and all participate in saturation, instability, and transport.
2. Eigenmode cross correlations, the nonlinear growth rate, and transport fluxes are temporally intermittent. The cross phases oscillate between nonlinearly locked states and rotation. Multiple cross correlations enter the growth rate and transport fluxes, making them highly bursty despite fixed driving gradients.
3. On average the cross correlations phase mix to zero. The growth rate and fluxes are then governed by the competition between autocorrelations of the growing and damped eigenmodes. These nearly balance, resulting in strongly reduced instability drive and transport. We hypothesize that the observed temporal intermittency is facilitated by transitional values of P_t. Stable eigenmodes are important in saturation and transport, but none is sufficiently strong to acquire the hegemony characteristic of CTEM turbulence.

ACKNOWLEDGMENT

This work was supported by the U.S. Department of Energy under Grant No. DE-FG02-89ER-53291.

[1] L. D. Landau and E. M. Lifshitz, *Statistical Physics* (Pergamon, Oxford, 1980), pp. 451–452.
[2] R. H. Berman, D. J. Tetreault, T. H. Dupree, and T. Boutros-Ghali, Phys. Rev. Lett. **48**, 1249 (1992).
[3] P. W. Terry, P. H. Diamond, and T. S. Hahm, Phys. Fluids B **2**, 2048 (1990).
[4] S. Hirshman and K. Molvig, Phys. Rev. Lett. **42**, 648 (1979).
[5] D. Biskamp and A. Zeiler, Phys. Rev. Lett. **74**, 706 (1995).
[6] J. F. Drake, A. Zeiler, and D. Biskamp, Phys. Rev. Lett. **75**, 4222 (1995).
[7] B. D. Scott, Phys. Fluids B **4**, 2468 (1992).
[8] S. C. Cowley, R. M. Kulsrud, and R. Sudan, Phys. Fluids B **3**, 2767 (1991).
[9] F. Jenko, W. Dorland, M. Kotschenreuther, and B. N. Rogers, Phys. Plasmas **7**, 1904 (2000).
[10] A. Smolyakov, P. Diamond, and Y. Kishimoto, Phys. Plasmas **10**, 3826 (2002).
[11] D. A. D'Ippolito and J. R. Myra, Phys. Plasmas **9**, 4029 (2003).
[12] K. Itoh, S.-I. Itoh, and A. Fukuyama, *Transport and Structural Formation in Plasmas* (Institute of Physics, Bristol, 1999).
[13] P. W. Terry, J. N. Leboeuf, P. H. Diamond, D. R. Thayer, J. E. Sedlak, and G. S. Lee, Phys. Fluids **31**, 2920 (1988).
[14] L. M. Smith and F. Waleffe, Phys. Fluids **11**, 1608 (1999).
[15] L. M. Smith and F. Waleffe, J. Fluid Mech. **451**, 145 (2002).
[16] S. Boldyrev, Astrophys. J. **626**, L37 (2005).
[17] F. A. Haas and A. Thyagaraja, Phys. Rep. **143**, 240 (1986).
[18] D. A. Baver, P. W. Terry, and E. Fernandez, Phys. Lett. A **267**, 188 (2000).
[19] D. A. Baver, P. W. Terry, and R. Gatto, Phys. Plasmas **9**, 3318 (2002).
[20] V. Sokolov and A. K. Sen, Phys. Rev. Lett. **92**, 165002 (2004).
[21] P. W. Terry, Phys. Rev. Lett. **93**, 235004 (2004).
[22] P. W. Terry, R. Gatto, and D. A. Baver, Bull. Am. Phys. Soc. **49**, 82 (2004).
[23] P. W. Terry, R. Gatto, and D. A. Baver, Phys. Rev. Lett. **89**, 205001 (2002).
[24] R. Gatto, P. W. Terry, and D. A. Baver, Phys. Plasmas **13**, 022306 (2006).
[25] A. I. Smolyakov, P. H. Diamond, and M. Malkov, Phys. Rev. Lett. **84**, 491 (2000).
[26] B. A. Carreras, D. E. Newman, B. Ph van Milligen, and C. Hidalgo, Phys. Plasmas **6**, 485 (1999).
[27] D. E. Newman, B. A. Carreras, P. H. Diamond, and T. S. Hahm, Phys. Plasmas **3**, 1858 (1996).